

Federated Learning and Differential Privacy Techniques on Multi-hospital Population-scale Electrocardiogram Data

Vikhyat Agrawal

IIT Bombay

Mumbai, Maharashtra, India

200260058@iitb.ac.in

Sunil Vasu Kalmady

University of Alberta

Edmonton, Canada

kalmady@ualberta.ca

Venkataseetharam Manoj

Malipeddi

IIT Kharagpur

Kharagpur, India

Manisimha Varma Manthena

University of Alberta

Edmonton, Canada

Weijie Sun

University of Alberta

Edmonton, Canada

Saiful Islam

University of Alberta

Edmonton, Canada

Abram Hindle

University of Alberta

Edmonton, Canada

Padma Kaul

University of Alberta

Edmonton, Canada

Russell Greiner

University of Alberta

Edmonton, Canada

ABSTRACT

This research paper explores ways to apply Federated Learning (FL) and Differential Privacy (DP) techniques to population-scale Electrocardiogram (ECG) data. The study learns a multi-label ECG classification model using FL and DP based on 1,565,849 ECG tracings from 7 hospitals in Alberta, Canada. The FL approach allowed collaborative model training without sharing raw data between hospitals, while building robust ECG classification models for diagnosing various cardiac conditions. These accurate ECG classification models can facilitate the diagnoses while preserving patient confidentiality using FL and DP techniques. Our results show that the performance achieved using our implementation of the FL approach is comparable to that of the pooled approach, where the model is trained over the aggregating data from all hospitals. Furthermore, our findings suggest that hospitals with limited ECGs for training can benefit from adopting the FL model compared to single-site training. In addition, this study showcases the trade-off between model performance and data privacy by employing DP during model training. Our code is available at <https://github.com/vikhyatt/Hospital-FL-DP>.

KEYWORDS

Federated Learning, Differential Privacy, Electrocardiogram Data, ECG, EKG, Multi-hospital data, Healthcare, Machine Learning

1 INTRODUCTION

Electrocardiograms (ECGs), capturing the heart's electrical activity, offer critical insights into cardiac function, making them an indispensable diagnostic and monitoring tool for healthcare professionals in cardiology. As this test is non-invasive, painless, and

Permission to make digital or hard copies of all or part of this work for personal or classroom use is granted without fee provided that copies are not made or distributed for profit or commercial advantage and that copies bear this notice and the full citation on the first page. Copyrights for components of this work owned by others than the author(s) must be honored. Abstracting with credit is permitted. To copy otherwise, or republish, to post on servers or to redistribute to lists, requires prior specific permission and/or a fee. Request permissions from permissions@acm.org.

Accepted for ICMHI'24, May 17–19 2024, Yokohama, Japan

© 2024 Copyright held by the owner/author(s). Publication rights licensed to ACM.

quick, it is a popular diagnostic tool in clinical settings, and is used to diagnose a range of cardiac conditions, including arrhythmias, conduction disorders, and other anomalies [1–5]. Recent studies show that ECGs can identify and diagnose non-cardiac medical conditions, including but not limited to diabetes and Alzheimer's disease [6–8]. The manual analysis of ECG signals is a meticulous and error-prone task, even for seasoned specialists [9]. Consequently, developing accurate ECG classification models is critical for the prompt and precise detection of cardiac conditions, which is vital for effective treatment and management. This necessity has spurred the adoption of deep learning techniques to leverage the full potential of ECG data. By automatically learning hierarchical representations from raw ECG signals, deep neural networks can uncover intricate features that might elude traditional handcrafted algorithms. Recent years have witnessed notable advancements in Machine Learning models for diagnosing diseases through ECG data. Employing various learners, including Convolutional Neural Networks (CNNs) [10], Recurrent Neural Networks (RNNs) and their variants [11], these learned models, particularly CNNs and their derivatives, excel in identifying spatial patterns, waveforms, and morphological features linked to specific medical conditions. Applying these deep learning techniques improves ECG classification accuracy, advancing cardiac diagnostics.

However, building such models requires access to substantial and diverse datasets that represent different patient populations and medical contexts. Data acquisition from multiple healthcare institutions is crucial to achieving generalizable models across various clinical and demographic populations. This maximizes model performance for the collaborating hospitals and solves the problems that may arise from having less training data. It provides a well-performing local model for a hospital for data from various clinical and demographic groups [12–14]. However, the acquisition of ECG data from many hospitals introduces intricate challenges and privacy considerations. The autonomous nature of hospitals leads to many different data formats, recording systems, and ECG acquisition protocols. Additionally, certain healthcare facilities may cater exclusively to specialized clinical cohorts or serve geographically confined populations. For instance, a predictive model optimized

for a large urban hospital's patient data, might perform less effectively when applied to the data from a small rural clinic, where the patient population and health issues differ significantly. Consequently, a model derived from one hospital's dataset might not work for another hospital's dataset due to the presence of covariate shifts across datasets from disparate institutions. A covariate shift between two hospitals' data denotes a dissimilarity in patient characteristics, such as demographic features or disease prevalence, between the training dataset utilized for model development and the dataset encountered during deployment, potentially resulting in a decline in model performance.

Addressing privacy is an important concern, as hospitals are bound by a mandate to safeguard patient confidentiality and uphold ethical principles [47–49]. Recent research has additionally demonstrated that ECGs can be leveraged for biometric authentication, showcasing their capacity to discern and verify individuals [15, 16]. Furthermore, given the heightened sensitivity and confidentiality of medical data, specific individuals may be reluctant to provide their data to a central data collection [17, 18]. The indiscriminate sharing of raw ECG data may inadvertently compromise sensitive information, eroding trust. Thus, the establishment of collaborative, privacy-centric data-sharing frameworks assumes paramount significance, with innovative methodologies such as Federated Learning (FL) and Differential Privacy (DP) emerging as promising solutions. This paper explores the application of FL and DP techniques on population-scale ECG data to develop accurate and robust ECG classification models while preserving data privacy and security. Sections 1.1 and 1.2 of this paper provides an overview of FL and DP, along with outlining the study's objectives. Section 2 then delves into related literature, exploring FL and DP applications in different healthcare contexts, especially for ECG data. We critically assess the limitations of prior work and highlight our contributions. Section 3 outlines the methods employed, discussing the prediction task, patient characteristics, learning algorithm, and the evaluation scheme. Section 4 presents the results derived from various experiments conducted related to both FL and DP. Section 5 interprets our work and summarizes the entire paper.

1.1 Federated Learning

Federated Learning (FL) is a pioneering paradigm designed to address the multifaceted challenges associated with learning from many data sources in a way that preserves privacy [20]. This new method allows one model to be trained together using data from different sources, like hospitals, without sharing private information. Each hospital helps improve that single model through minor updates while keeping sensitive details private. FL ensures that each hospital's data stays within its boundaries, preserving data privacy and security. Figure 1 depicts the FL configuration employed in our multi-hospital setup. FL is a multi-step process in which each hospital initially preprocesses its local ECG data, a crucial step to ensure data consistency and implement privacy-preserving techniques, such as data anonymization. Subsequently, each hospital learns its own localized ECG classification model, based on its preprocessed data. These individual models are then aggregated

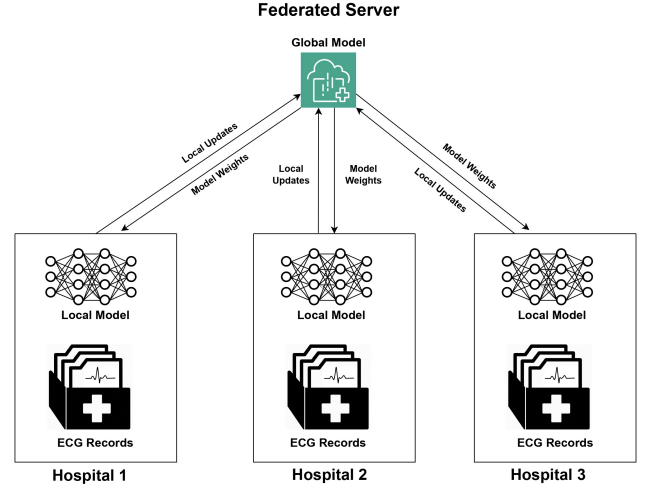


Figure 1: Diagram illustrating the Federated Learning setup for multi-hospital ECG datasets

into a global model through techniques such as federated averaging, which appropriately weighs each hospital's contribution. The global model is then transmitted back to the individual hospitals, where it undergoes fine-tuning in successive iterations, until it converges on a global ECG classification model. Through this approach, FL establishes itself as a solution for collaborative medical research across diverse healthcare institutions.

1.2 Differential Privacy

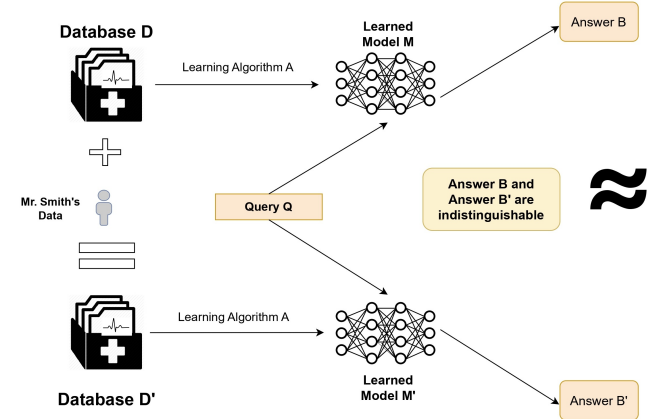


Figure 2: Diagram illustrating Differential Privacy

Differential privacy (DP), a fundamental concept in data privacy, has become a crucial framework for addressing the delicate balance between preserving data usefulness and safeguarding individual privacy. It constitutes a foundational construct in the context of data analysis, which frequently involves using sensitive personal information while adhering to stringent ethical and legal mandates safeguarding the privacy of individuals. Initially introduced by

Dwork et al. in 2006 [19], this framework has since gained significant prominence as it offers a robust mathematical guarantee of privacy protection within data analysis processes. By quantifying the extent to which the inclusion or exclusion of a single individual's data point influences the outcomes of data analyses, DP approaches ensure that the privacy of any individual remains effectively preserved. In doing so, it furnishes a rigorous means of protecting individual privacy and inspires confidence in data sharing and analysis, thus facilitating collaborative medical research and advancing healthcare outcomes. Figure 2 illustrates the DP setup in the context of machine learning. In this scenario, we can train 2 models using learner A: model M on database D and M' on database D', which is the dataset formed by adding Mr. Smith's data to dataset D. Subsequently, we pose the same query Q to both of these trained models. If the resulting answers, B and B', are indistinguishable, then no private information about Mr. Smith can be inferred.

1.3 Aim of Study

This study investigates the impact of incorporating FL and DP techniques in the analysis of ECG data obtained from 7 distinct hospitals located in Edmonton, Alberta, Canada. Our prediction task is to develop an ECG classification model that can use a patient's ECG to determine if that patient has zero or more of several prevalent cardiovascular and metabolic diseases. The overarching goal is to investigate whether adopting a federated approach with (versus without) differential privacy can enhance data privacy and security without significantly compromising the performance of pre-existing global models.

2 RELATED WORK

Various studies have explored the implementation of FL in healthcare applications. One such study by Raza et al. [21] employed an FL approach to categorize ECGs into 5 heartbeat categories on the MIT-BIH Dataset [22] focusing on model explainability. However, it uses data from a single hospital, undermining the fundamental justification for employing FL in this scenario. In contrast, our research overcomes this limitation by incorporating data aggregated from multiple hospitals. In a customized FL approach, Tang et al. [23] demonstrates enhanced performance in their FL model, personalized for each local node, compared to a model trained using the FedAvg algorithm. However, their focus — classifying ECGs into distinct heartbeat types — is designed to be relevant to the diseases under consideration. Additionally, their study would benefit from a comparative analysis across demographic groups and an inter-site performance evaluation. Our study used the same FedAvg algorithm in an inter-site analysis framework inspired by the work conducted by Goto et al. [24]. They developed FL models for hypertrophic cardiomyopathy classification by integrating ECGs and echocardiograms from 4 different hospitals, thereby setting a benchmark for assessing the utility of ECGs. We differ from the HCM-focused study [24] as we leverage ECG data to comprehensively diagnose various cardiovascular and metabolic diseases in patients — more details in Sections 3.1 and 3.2. Both Lin et al. [25] and Meqdad et al. [26] propose novel FL approaches for 5-class

heartbeat classification using ECGs, specifically beneficial for non-IID smart device data, with validation on the MIT-BIH dataset. The non-IID nature of the data in this context arises because the data from each node (patient or device) originates from the same patient, leading to a lack of independence and thus categorizing it as non-IID. In contrast to Lin et al. [25] and Meqdad et al. [26], Baumgartner et al. [27] learns a multi-label classification model that can detect 13 SNOMED codes using ECGs from 5 data sources [33], emphasizing metric-focused evaluations while using FL to preserve privacy for multi-site data. Ying et al. [34] introduces a pioneering preprocessing method for ECG data by converting ECGs to images and employs FL for smart devices, incorporating a semi-supervised approach with pseudo-labeling. Nevertheless, they conducted an analysis using the MIT-BIH dataset, known for its non-IID nature and utility for patient-level data nodes. Joshi, Pal et al. [35] provides a comprehensive review of prevailing FL approaches in healthcare until 2022. Finally, Dolo et al. [36] proposes for the Differentially Private Stochastic Gradient Descent applied to the Federated Averaging (DPSGDFedAvg) algorithm, specifically for diabetes prediction using the Pima Indian dataset. We adopt DPSGDFedAvg for our experiments using DP in Section 4.2.

This study adds to the existing body of literature by introducing several advancements, thus distinguishing itself from prior research. An essential point of distinction lies in the fact that numerous papers utilize ECG data from the MIT-BIH dataset sourced from a single hospital. In these cases, FL is implemented on an individual patient level, treating them as nodes, and the data is non-IID. In contrast, our approach uses hospitals as nodes in our FL model, mirroring a more realistic deployment scenario. Our model utilizes data from 7 hospitals in Edmonton, Alberta, Canada, where each hospital contains data from numerous patients. The linkage of our ECG dataset to provincial administrative health records provides multiple diagnostic labels based on ICD-10 coding systems, meaning our learned models can predict many more labels than others that incorporate private data from multiple sources [23, 27]. Our study ensures a substantial number of instances for each disease type, with a minimum of 15,000 instances for the least prevalent disease, facilitating ample training samples. Additionally, a distinctive characteristic of our machine learning approach is that our learned model will simultaneously predict the diagnosis of multiple diseases for a given ECG instance. We employ the FedAvg algorithm for FL, consistent with the existing literature, considering its established efficacy. Furthermore, we introduce an additional layer of data privacy by incorporating the Differential Privacy Stochastic Gradient Descent (DP-SGD) algorithm [37] during FL training. The inclusion of DP-SGD is a novel aspect absent in previous related works on similar prediction tasks and aligns with contemporary privacy norms and legal requirements. Additionally, our research conducts intersite analysis, addressing a notable gap in some previous literature. This analysis underscores the motivation behind employing FL, particularly for hospitals with limited ECG data, thus ensuring both efficacy and data privacy simultaneously, a crucial aspect not explored in earlier studies. Furthermore, we aim to demonstrate that the effective implementation of the FL approach is influenced by factors such as the distribution of disease prevalence among different hospitals, the age-sex distribution, and the number

Table 1: ECG distribution among hospitals

Site \ Data Split	Train	Tuning	Holdout
Hospital 1	232517	59142	195383
Hospital 2	217578	54774	180733
Hospital 3	98865	25323	81938
Hospital 4	87201	21436	72442
Hospital 5	78329	20420	65035
Hospital 6	19769	5184	16334
Hospital 7	13714	3261	11291
TOTAL	747973	194720	623156

of ECGs available in these hospitals. In addition, this study seeks to showcase the trade-off between model performance and data security by employing DP techniques in model training.

3 METHODS

3.1 Data Description and Patient Characteristics

This work used a dataset comprising 2,015,808 ECG records from 260,065 patients, collected between February 2007 and April 2020, containing 14 hospitals in Edmonton, Alberta, Canada. We have implemented identical ECG data preprocessing methods as outlined in the Analysis Cohort subsection of the Methods section in Sun et al. [38]. An ECG record was labeled with ICD-10 codes of the healthcare episode if its acquisition date fell within the timeframe of the episode. After excluding ECGs that could not be linked to any episode, those of patients below 18 years of age, and ECGs with poor signal quality, our analysis cohort comprised 1,603,109 ECGs originating from 748,773 episodes involving 244,077 patients [38].

Table 1 provides the distribution of ECGs across various hospitals along with different experimental splits. We have set a training dataset quota of 12,500 ECGs per hospital for model development—meaning our training set, used to train our Federated Learning-based model, included just 7 hospitals. The final dataset consists of 1,565,849 ECGs, encompassing 243,128 patients. This study employs standard 12-lead ECG tracings derived from the Philips IntelliSpace ECG system, consisting of voltage-time series, sampled at a rate of 500 Hz over a duration of 10 seconds for each of the 12 leads, resulting in a total of $500 \times 10 \times 12$ voltage measurements per ECG. General patient characteristics have been described by Sun et al. [38], and hospital-wise distributions are presented in Table 2 and Table 3.

3.2 Prediction Task

Our dataset, sourced from Alberta Health Services (AHS), contains administrative electronic health records (EHRs) and ECGs. Based on linkage of ECGs to administrative health records, we labeled each ECG with the set of ICD-10 diagnosis codes assigned to this patient. The objective of our research is a multi-label classification task that uses both ECG waveforms and demographic data to predict the probabilities of 10 specific diseases, as defined by their respective ICD-10 codes (see Table 6). We chose these classification

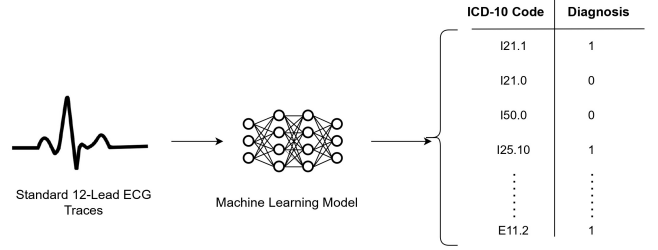


Figure 3: Diagram depicting the prediction task by representing the output using a specific example

labels because of their significant clinical relevance to cardiovascular and metabolic diseases and their widespread prevalence across diverse demographic cohorts, as elucidated by the research findings presented by Sun et al. [38]. Figure 3 provides an example of the predictions generated by our model. The model predicts each disease label independently, assigning either 0 (negative) or 1 (positive) for a given ECG tracing as input. Our dataset aggregates information from multiple hospitals, so our approach involves developing a multi-label model within a federated learning framework. We compare the standard and federated learning models to discern the efficacy of federated learning in this context. Finally, we will compare models trained and tested independently within and across each participating hospital, evaluating their performance.

3.3 Learning Algorithm

For the Deep Learning (DL) model, we implemented a CNN based on the residual neural network architecture, consisting of a convolutional layer, 4 residual blocks with 2 convolutional layers per block, followed by a dense layer (total of 8,922,644 model parameters) [38]. We used batch normalization [45], ReLU [44], and dropout after each convolutional layer. Each ECG instance was loaded as a 12×5120 numeric matrix. Additional features such as age and sex were passed to a 10-hidden-unit layer and concatenated with the dense layer, and finally passed to a softmax layer to produce the outputs. Binary cross-entropy was used as the loss function with the initial learning rate of 10^{-3} , Adam optimizer [46], ReLU activation function, kernel size of 16, batch size of 512, and dropout rate of 0.2 with other hyper-parameters set to default. Models were learnt for a maximum of 50 epochs. The learning rate was reduced to 10^{-5} if there was no improvement in tuning loss for 7 consecutive epochs, and the learning process was stopped if loss in the tuning set did not reduce for 9 epochs. We trained all our models on the NVIDIA Driver version 418.88 with 8 Tesla V100-SXM2 GPUs and 32 GB of RAM per GPU. Each DL model took approximately 30 min per epoch to train.

3.4 FL/DP Algorithm

3.4.1 Federated Averaging (FedAvg)

We implemented the Federated Averaging (FedAvg) algorithm [20], a decentralized machine learning paradigm designed for training models across various hospitals while ensuring data privacy. In the FedAvg framework, each participating hospital autonomously conducts model training on its locally stored ECG data. Instead

Table 2: Patient Characteristics

Hospital	1	2	3	4	5	6	7
Number of ECGs	487042	453085	206126	181079	163784	41287	28266
Median Age (min-max)	66 (18 - 108)	66 (18 - 108)	69 (18 - 106)	71 (18 - 108)	71 (18 - 108)	64 (18 - 105)	72 (18 - 107)
Male %	59.66	58.24	55.77	50.61	54.13	53.40	52.20

Table 3: Prevalences of classification labels and comorbidities

Hospital	1	2	3	4	5	6	7
Prevalence of ICD-10 Classification Labels							
I21.1	16417 (3.37%)	19999 (4.41%)	4786 (2.32%)	3131 (1.73%)	3972 (2.43%)	615 (1.49%)	394 (1.39%)
I21.0	14329 (2.94%)	16840 (3.72%)	3022 (1.47%)	2250 (1.24%)	2859 (1.75%)	436 (1.06%)	274 (0.97%)
I50.0	78074 (16.03%)	62743 (13.85%)	23251 (11.28%)	21970 (12.13%)	19721 (12.04%)	2467 (5.98%)	3818 (13.51%)
I25.10	118240 (24.28%)	125316 (27.66%)	33251 (16.13%)	27869 (15.39%)	33001 (20.15%)	3819 (9.25%)	3573 (12.64%)
I48.9	52394 (10.76%)	49914 (11.02%)	14291 (6.93%)	15671 (8.65%)	14132 (8.63%)	2161 (5.23%)	2447 (8.66%)
I21.4	47306 (9.71%)	46823 (10.3%)	25162 (12.21%)	17054 (9.42%)	19789 (12.08%)	2011 (4.87%)	2286 (8.09%)
I48.0	55344 (11.36%)	30892 (6.82%)	17753 (8.61%)	17041 (9.41%)	12924 (7.89%)	1145 (2.77%)	1767 (6.25%)
E87.5	14263 (2.93%)	10635 (2.35%)	3220 (1.56%)	2788 (1.54%)	1841 (1.12%)	413 (1.00%)	635 (2.25%)
E11.2	22683 (4.66%)	21745 (4.80%)	6680 (3.24%)	4305 (2.38%)	4106 (2.51%)	631 (1.53%)	492 (1.74%)
I35.0	14207 (2.92%)	6799 (1.50%)	1914 (0.93%)	2066 (1.14%)	1827 (1.12%)	163 (0.39%)	232 (0.82%)
Prevalence of Comorbidities							
Peripheral Vascular Disease	7184 (1.48%)	3393 (0.75%)	19582 (9.50%)	1504 (0.83%)	1262 (0.77%)	151 (0.37%)	194 (0.69%)
Cerebrovascular Disease	28453 (5.84%)	7684 (1.70%)	7992 (3.88%)	3516 (1.94%)	3525 (2.15%)	802 (1.94%)	729 (2.58%)
Myocardial Infarction	113887 (23.38%)	120451 (26.58%)	37501 (18.19%)	30539 (16.87%)	36440 (22.25%)	4011 (9.71%)	4424 (15.65%)
Hypertension	42189 (8.66%)	36162 (7.98%)	18944 (9.19%)	13852 (7.65%)	14653 (8.95%)	2244 (5.44%)	3037 (10.74%)
Dementia	7624 (1.57%)	8421 (1.86%)	3604 (1.75%)	5137 (2.84%)	3248 (1.98%)	149 (0.36%)	690 (2.44%)
Chronic Pulmonary Disease	28407 (5.83%)	34426 (7.60%)	15136 (7.34%)	16337 (9.02%)	16034 (9.79%)	3469 (8.40%)	3271 (11.57%)
Renal Disease	9799 (2.01%)	4466 (0.99%)	1781 (0.86%)	1718 (0.95%)	1634 (1.00%)	202 (0.49%)	359 (1.27%)
Liver Disease	8706 (1.79%)	5233 (1.15%)	1530 (0.74%)	1631 (0.90%)	1172 (0.72%)	221 (0.54%)	197 (0.70%)
Cancer	40575 (8.33%)	24215 (5.34%)	9437 (4.58%)	8294 (4.58%)	5887 (3.59%)	671 (1.63%)	1223 (4.33%)

of transmitting raw data to a central server, only the model updates, typically in the form of gradients, are communicated. The central server aggregates these updates and computes a global model through parameter averaging. Subsequently, the resulting global model is disseminated to the participating hospitals, initiating a recurrent iterative process. FedAvg is particularly beneficial in scenarios marked by distributed ECG data across multiple sites, enabling collaborative model training without explicit data exchange.

3.4.2 Differentially Private Stochastic Gradient Descent (DP-SGD). To implement differential privacy during model training, we have employed the Differential Privacy Stochastic Gradient Descent (DP-SGD) algorithm [37]. This advanced optimization technique is specifically tailored for machine learning models, primarily focusing on integrating differential privacy guarantees. DP-SGD extends the traditional Stochastic Gradient Descent (SGD) optimization algorithm by introducing mechanisms that introduce controlled noise into gradient computations. This approach is particularly effective in mitigating the risk of extracting sensitive information, such as patient details, from the ECG data. The intentional addition of noise ensures that the model's updates maintain differential privacy, whereby the inclusion or exclusion of any single ECG has a negligible impact on the overall model parameters. DP-SGD strikes

a balance between optimizing model performance and upholding the privacy of patient information within the ECG data. We have incorporated DP-SGD into our framework utilizing the Opacus library [29], which employs the Rényi Differential Privacy [30, 31] accountant as its mechanism for tracking privacy.

3.5 Evaluation

We split the ECG dataset into different groups for training the models and evaluating models. We randomly split the ECGs by disjoint patients into the development set (60%) and holdout set (40%). In the development set, we split into 80% for training and 20% for tuning the model's performance during development. The proportions were maintained approximately within each hospital site for the previously mentioned split. The holdout set was kept aside to independently test the model. To mitigate the bias, we made sure that ECGs from the same patient were not used in both the development and holdout sets. The metric we reported was based on this holdout set, particularly the area under the receiver operating characteristic curve (AUROC) [39], also known as the C-index. For each of the 10 ICD codes corresponding to specific medical diagnoses, we conducted individual calculations of the AUROC values. Subsequently, we computed the macro AUROC score encompassing all diseases. This iterative process was repeated

1000 times through repeated random sampling, involving 10% of the testing data on each occasion. Following collecting macro AUROCs from these iterations, we calculated the mean of the 1000 macro AUROCs and determined the 95% confidence intervals using the percentile method. We use these 95% confidence intervals to discern statistical significance in our results.

4 RESULTS

In this section, we present the results from our analysis of patient characteristics and the experiments conducted for our diagnosis task using FL and DP. Table 2 and Table 3 present the distribution of age, sex, common comorbidities and diagnostic classes in the study cohort across the hospitals, highlighting their differences. Hospitals 1 and 2 consistently exhibit the highest prevalence percentages among all participating healthcare facilities for most classification labels. Moreover, the distribution of gender and age across all hospitals is notably varied. Hospitals 4, 5, and 7 exhibit a higher median age range of 71-72 years, which is 5 to 8 years greater compared to Hospitals 1, 2, and 4, where the median age ranges from 64 to 66 years. Similarly, Hospitals 1 and 2 have a relatively higher percentage of men (58-59%) compared to Hospital 4, which maintains an equal gender distribution with 50% men and 50% women. All comorbidities and diagnostic classes also showed significant variations in their prevalence rates across the hospitals. Noteworthy variations are observed in the prevalence rates of specific comorbidities, with Peripheral Vascular Disease exhibiting a significantly higher prevalence in Hospital 3 (9.50%) compared to other hospitals (with a maximum of 1.48%). Conversely, the prevalence of Cancer, Dementia, Heart Failure (I50.0), Paroxysmal Atrial Fibrillation (I48.0), and Myocardial Infarction is conspicuously lower in Hospital 6 in comparison to its counterparts.

4.1 Results from Federated Learning

In this section, we examine the outcomes resulting from the FL model training process on our dataset. Note that, from this point onward, we refer to hospitals as sites in this section. Initially, we employed a conventional approach, where the entire development dataset (training and tuning ECGs from all the hospitals) was utilized to train a single ECG classification model. This model will serve as our benchmark for evaluation, as we aim to attain comparable performance using an FL setup. Subsequently, we implemented a DL model with a similar architecture within the framework of FL. We then conducted a comparative analysis of the results obtained from both models using the holdout dataset (holdout ECGs from each of the hospitals, as well as the entire holdout set). For reference, we will denote the first approach as the "standard approach" method and the second as the "FL approach."

As depicted in Table 4 below, we conducted a comparative analysis of models trained using 2 distinct methodologies. The first row outlines the model's performance when trained under the conventional approach, which involves centralizing all data for model training. Subsequently, the second row illustrates the model's performance when trained using the FL approach. We observe that specific sites, such as Site 7, exhibit low performance even when employing the Standard approach. It is also noteworthy that a marginal reduction in performance is observed with the adoption of the FL approach as

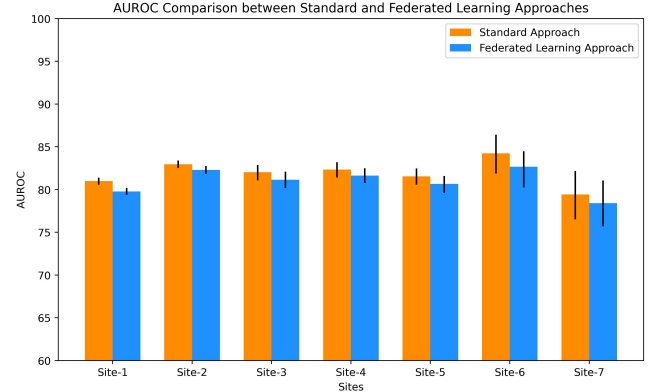


Figure 4: Comparison of Model Performance (AUROC in %) between the Federated Learning (FL) Approach and Standard Approach for different sites. The error bars on the graph indicate the 95% confidence intervals.

opposed to the conventional data aggregation technique. Furthermore, the performance difference between the standard approach model and the FL approach model is statistically significant only for Site 1's test data, while the test performance on data from all other hospitals is not statistically different. Nonetheless, it is crucial to acknowledge that the FL method brings substantial benefits in strengthening data security and ensuring privacy as described by Yin et al. [28]. The results are presented graphically in Figure 4, given by the data provided in Table 4. It is essential to highlight that Figure 4 represents the mean of the Macro AUROCs derived from the testing dataset, accompanied by their corresponding 95% confidence intervals. The rationale behind choosing macro AUROC over label-wise performance lies in its alignment with the trends observed in the class-wise AUROC scores (refer to Figures 7 and 8 in the Appendix). Utilizing a single value, the Macro AUROC simplifies summarizing the overall performance, avoiding the complexity of interpreting 10 distinct values. Moreover, we have observed from Table 3 and Figures 7 and 8 that there is no discernible relation between the prevalence of diseases and their corresponding AUROC scores.

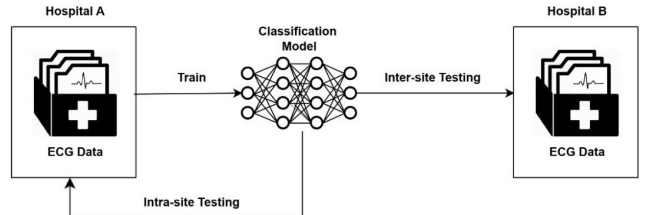


Figure 5: Diagram explaining the intra-site and inter-site testing framework. For intra-site testing, the classification model is trained and tested on Hospital A's respective train and test sets. In contrast, for inter-site testing, the model is trained on Hospital A's training data and tested on Hospital B's testing data

Table 4: AUROC scores of models trained in FL and Standard approach along with the respective 95% confidence intervals

Model \ Site	Site-1	Site-2	Site-3	Site-4	Site-5	Site-6	Site-7	Complete Test Data
Standard Approach	80.99 [80.58,81.39]	82.95 [82.52,83.39]	82.02 [81.07,82.90]	82.33 [81.42,83.20]	81.55 [80.57,82.48]	84.23 [81.88,86.42]	79.43 [76.52,82.18]	82.07 [81.58,82.50]
FL approach	79.78 [79.37,80.20]	82.29 [81.84,82.75]	81.14 [80.17,82.09]	81.63 [80.78,82.49]	80.65 [79.63,81.58]	82.66 [80.24,84.48]	78.40 [75.69,81.05]	81.03 [80.50,81.48]

Table 5: Table with intra-site and inter-site performance (AUROC in %) comparisons along with corresponding 95% confidence intervals

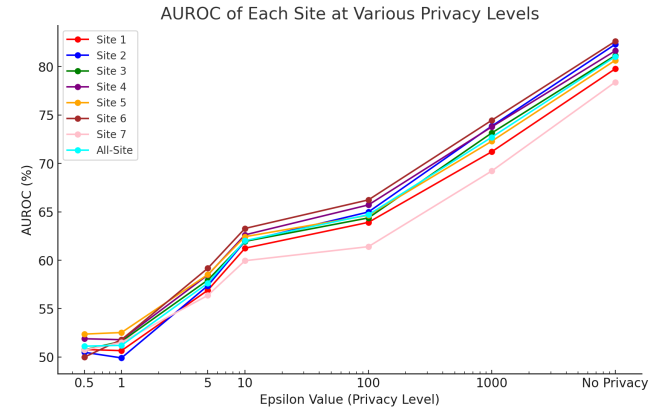
Train site / Test site	Site 1 (59,142)	Site 2 (54,774)	Site 3 (25,323)	Site 4 (21,436)	Site 5 (20,420)	Site 6 (5,184)	Site 7 (3,261)	Complete test data
Site 1 (232,517)	78.87 [78.41,79.29]	80.48 [79.97,80.98]	79.58 [78.55,80.53]	79.80 [78.90,80.73]	78.99 [77.87,80.08]	80.51 [77.87,83.03]	77.14 [73.82,80.04]	79.62 [79.12,80.09]
Site 2 (217,578)	78.70 [78.27,79.18]	81.61 [81.10,82.06]	80.41 [79.40,81.33]	80.54 [79.57,81.47]	79.76 [78.69,80.80]	82.39 [80.10,84.51]	77.18 [74.02,80.13]	80.08 [79.52,80.56]
Site 3 (98,865)	77.80 [77.36,78.22]	80.43 [79.96,80.90]	80.28 [79.36,81.17]	80.26 [79.34,81.19]	79.54 [78.50,80.49]	80.55 [77.70,83.15]	77.36 [74.20,80.05]	79.35 [78.86,79.82]
Site 4 (87,201)	76.94 [76.45,77.39]	79.71 [79.20,80.17]	78.89 [77.92,79.86]	80.04 [79.07,80.91]	78.87 [77.79,79.99]	81.42 [78.84,83.72]	77.38 [74.38,80.18]	78.57 [78.06,79.05]
Site 5 (78,329)	77.49 [77.05,77.91]	80.10 [79.62,80.60]	79.31 [78.37,80.25]	79.87 [78.87,80.83]	79.98 [78.95,80.97]	80.84 [78.20,83.20]	77.33 [74.16,80.04]	79.12 [78.61,79.62]
Site 6 (19,769)	73.04 [72.51,73.54]	75.64 [75.05,76.20]	75.01 [73.82,76.14]	75.90 [78.84,83.72]	75.19 [74.00,76.36]	78.82 [75.51,81.53]	73.14 [69.21,76.57]	74.64 [74.09,75.18]
Site 7 (13,714)	74.01 [73.52,74.50]	76.70 [76.17,77.21]	76.58 [75.46,77.60]	76.64 [75.54,77.73]	76.42 [75.30,77.55]	78.66 [75.59,81.28]	75.34 [72.43,78.44]	75.70 [73.90,77.49]
Complete Train Data	80.99 [80.58,81.39]	82.95 [82.52,83.39]	82.02 [81.07,82.90]	82.33 [81.42,83.20]	81.55 [80.57,82.48]	84.23 [81.88,86.42]	79.43 [76.52,82.18]	82.07 [81.58,82.50]

In the subsequent experiment, we conduct both intra-site and inter-site testing for our ECG classification model without utilizing FL. This experiment is designed to encourage the adoption of FL for training classification models. Figure 5 depicts the schematic representation of this experiment. A classification model is trained without FL on Hospital A and subsequently tested on data from Hospital B's testing dataset for inter-site testing. Conversely, for intra-site testing, the model is trained and tested on Hospital A's training and testing datasets, respectively. Table 5 offers a comprehensive overview of the performance of models trained utilizing data from individual sites. For instance, let us consider the cell denoted as (site-1, site-1) in the table. This specific cell represents the model's performance when trained using data exclusively from site-1 and subsequently tested on the test data originating from the same site. The last column of the table contains the model's overall performance on the entire test dataset. Similarly, the final row in the table presents the model's performance across various sites when trained on the entire training dataset. This row is the same as the standard approach in the previous experiment (Table 4).

A conspicuous pattern emerges from the presented table. The models trained on sites 6 and 7 demonstrate inferior performance compared to all models trained on data from the first 5 sites when tested on any of the 7 test sets. This may be attributed to the first 5 sites possessing significantly more number of ECG samples compared to sites 6 and 7. This does not imply that site-1 consistently achieves the best performance across all test sets, as the model trained on site-2 data exhibits superior performance in 4 out of the 7 test sets. Furthermore, the observed trend reveals a direct and proportional relationship between the model's performance and the origin of its training data with the exception of Sites 6 and 7. A model trained on site-A exhibits performance that matches those trained on other sites when tested on site-A data. For instance, a model trained on site-5 training data performs noticeably worse than other models when tested on datasets other than the site-5 testing dataset. However, when tested on site-5 data, its performance is marginally better to any of the other models. However, a diminishing performance trend is evident in other sites as their respective training dataset sizes decrease. When comparing the performance

of models trained individually for each site with those trained using the standard approach with the complete train dataset, a clear pattern emerges. In the majority of instances, the standard approach model surpasses its individually trained counterparts. This trend underscores the significant advantages of adopting the FL approach, as it consistently enhances the model's performance across most cases. Particularly, hospitals with smaller sample sizes experience a marked improvement in their model performance, in stark contrast to hospitals with larger sample sizes, which exhibit a more modest impact.

4.2 Results from Differential Privacy

**Figure 6: Plot shows model performance for different values of epsilon (tested on data from different sites)**

In our experiment with DP, we investigate the impact of incorporating DP on our model's performance. Our attention shifts to the model training process, employing the FL approach and integrating DP at the site level. During the local training phase within this FL context, we implemented DP-SGD for parameter updates. As noted in Section 1.2, the parameter ϵ in DP measures the privacy guarantees provided by the algorithm. A smaller value of ϵ signifies a stronger privacy guarantee, implying that less information about

a specific individual can be inferred from the output. It fine-tunes the balance between data utility and individual privacy when implementing DP. Thus, as privacy in DP is quantified using ϵ , we varied this parameter to observe its influence on model performance.

During our testing with different ϵ values in the DP-SGD technique, we observed a noticeable pattern (see Figure 6). It became evident that the model's performance exhibited a diminishing trend as we reduced the ϵ value. The model performances approached AUROC levels akin to random guessing, with values close to 0.5, for ϵ values below 1. ϵ serves as a pivotal element in DP, as it governs the extent of noise added to the gradient updates during training. As we lower ϵ , a more stringent level of privacy protection is achieved, accompanied by increased noise injection. However, we have observed from our experiments that this heightened privacy protection comes at the cost of reduced model performance.

5 DISCUSSION

Our analytical framework comprises 2 distinct components: FL and DP. In the FL framework, we benchmarked our model performance against standard models devoid of the FL technique. Our findings indicate that FL model performance registers a negligible decrease (< 2%) across all sites, concurrently ensuring robust data security and privacy. During inter-site testing, we also observed advantageous outcomes for hospitals with limited data under the FL paradigm. This advantage may be due to the potential inclusion of rare disease occurrences in datasets from hospitals with more extensive ECG collections. We also note that models trained using the standard approach on sites with many ECGs (e.g., Site 1 and Site 2) demonstrate good performance when tested across all sites, including those with fewer ECGs. Furthermore, we observe a direct correlation between the origin of training data and model performance. Models perform well when trained and tested on the same site, as displayed by a model trained on Site 5 data and tested on Site 5 data, exhibiting comparable performance to models tested on other sites for the corresponding testing data. Moreover, our model shows increased robustness within the FL framework, owing to its training across disparate datasets with varying demographics and prevalence rates. This adaptability enhances the model's generalization capacity, fostering resilience to variations in data.

In the DP experiment, the DP-SGD algorithm was employed, revealing a discernible correlation between the value of ϵ and the model performance. As ϵ increases, indicating a decrease in privacy, a concurrent increase in model performance is observed—an anticipated outcome. The trade-off between privacy and utility becomes more pronounced with diminishing ϵ values. While the augmented noise levels enhance privacy safeguards, they also diminish the model's ability to discern subtle patterns and features in the data. Consequently, the model's performance deteriorates when ϵ values are reduced, manifesting as reduced accuracy and predictive capability. This observation underscores the fundamental trade-off that must be considered in applications of differential privacy: increasing privacy constraints may augment utility at the potential expense of privacy, whereas augmenting privacy protection can lead to compromised model performance. Therefore, the selection of epsilon values should align with the project's specific

privacy requirements and performance objectives. Ponomareva et al. [40] posits that maintaining an epsilon value below 10 provides a substantiated privacy assurance. The assertion is supported by empirical evidence derived from real-world datasets and machine-learning models.

Recent research has suggested alternative methodologies for conducting federated averaging on non-independent and identically distributed (non-IID) data [41–43]. Despite exploring these advanced models beyond FedAvg in domains such as healthcare, we used FedAvg as a baseline model for this study. This decision is based on its role in evaluating the initial feasibility of retaining the FL approach, recognizing the preliminary nature of our investigation into this specific topic. Our choice of labels in the methods section was driven by thoughtful consideration of ICD-10 codes associated with cardiovascular and metabolic conditions of clinical importance. The decision-making process was informed by ECG-based predictability of selected cardiovascular ICD-10 codes [6], and sufficient representation across various hospital sites. However, we acknowledge the representative nature of our label selection and highlight the need for future experiments to explore if similar trends extend to other diagnostic categories. The use of ECG machines from a single manufacturer to capture all ECG data in this study presents a potential limitation. Employing ECG equipment from a singular manufacturer restricts the diversity of instrumentation and may limit the generalizability and external validity of the study's findings. However, the examination of ECG cohorts reveal notable variations in age, sex and disease prevalence rates across the 7 hospitals despite their geographical proximity and single healthcare provider (Table 2 and Table 3). These observed variations in clinical and demographic distributions among hospitals underscore the importance for adopting FL approaches for developing robust and equitable prediction models.

The imperative for rigorous adherence to regulatory frameworks in healthcare, exemplified by the Health Insurance Portability and Accountability Act (HIPAA) in the United States and the General Data Protection Regulation (GDPR) in the European Union, underscores the importance of implementing FL and DP models for diagnosis tasks. Given the sensitive nature of health data and the potential for significant privacy breaches, compliance with such regulations is not merely a legal obligation but a fundamental ethical consideration. Against this backdrop, FL emerges as a pivotal research area with its inherent focus on decentralized model training and DP. This study seeks to explore and contribute to the intersection of FL and DP, aiming to enhance ECG ML models' robustness and privacy assurances in compliance with prevailing legal frameworks. DP-SGD offers several noteworthy advantages in ML and data privacy. First and foremost, its incorporation of gradient clipping and noise addition as defense mechanisms against data poisoning significantly enhances the resilience of ML models. By constraining gradients and introducing controlled noise, DP-SGD mitigates the risk of adversarial influence on the training process, ultimately leading to more reliable and robust models. Moreover, DP-SGD's ability to safeguard against privacy breaches, including membership inference attacks, through strategic noise injection is a crucial feature. The strategic noise injection ensures the privacy of individuals' data

and hinders malicious actors from inferring sensitive information, thereby reinforcing privacy protections. These advantages position DP-SGD as a valuable tool in addressing the twin challenges of data poisoning and privacy breaches in machine learning. However, it is essential to acknowledge certain limitations associated with DP-SGD. One prominent concern is the trade-off between privacy and utility. The introduction of noise into the gradient updates, although essential for privacy protection, can reduce the model's overall accuracy and performance. Striking the right balance between preserving privacy and maintaining a high level of utility remains a complex and ongoing challenge. One potential approach for determining the optimal value of ϵ in the context of DP might be employing Membership Inference Attacks [32] to evaluate the effectiveness of the privacy measures. Additionally, the computational overhead incurred by DP-SGD is non-negligible. The process of computing and adding noise to gradients can significantly increase the training time and resource requirements, which can be a practical concern in applications where real-time or high-throughput processing is critical. Therefore, practitioners and researchers must carefully consider these trade-offs and make informed decisions when implementing DP-SGD in their machine learning workflows. Nonetheless, the benefits of DP-SGD in terms of privacy preservation and robustness make it a compelling approach, with its limitations being areas for continued refinement and innovation in privacy-preserving machine learning.

REFERENCES

- Shashikumar, S., Shah, A., Li, Q., Clifford, G. & Nemati, S. A deep learning approach to monitoring and detecting atrial fibrillation using wearable technology. *2017 IEEE EMBS International Conference On Biomedical & Health Informatics (BHI)*. pp. 141-144 (2017)
- Serhani, M., T El Kassabi, H., Ismail, H. & Nujum Navaz, A. ECG monitoring systems: Review, architecture, processes, and key challenges. *Sensors (Basel)*. **20**, 1796 (2020,3)
- ŞEN, S. & ÖZKURT, N. ECG Arrhythmia Classification By Using Convolutional Neural Network And Spectrogram. *2019 Innovations In Intelligent Systems And Applications Conference (ASYU)*. pp. 1-6 (2019)
- Liu, X., Wang, H., Li, Z. & Qin, L. Deep learning in ECG diagnosis: A review. *Knowl. Based Syst.* **227**, 107187 (2021,9)
- Somani, S., Russak, A., Richter, F., Zhao, S., Vaid, A., Chaudhry, F., De Freitas, J., Naik, N., Miotto, R., Nadkarni, G., Narula, J., Argulian, E. & Glicksberg, B. Deep learning and the electrocardiogram: review of the current state-of-the-art. *Europace*. **23**, 1179-1191 (2021,8)
- Sun, W., Kalmady, S., Salimi, A., Sepehrvand, N., Ly, E., Hindle, A., Greiner, R. & Kaul, P. ECG for high-throughput screening of multiple diseases: Proof-of-concept using multi-diagnosis deep learning from population-based datasets. (arXiv,2022)
- Lou, Y., Lin, C., Fang, W., Lee, C., Wang, C. & Lin, C. Development and validation of a dynamic deep learning algorithm using electrocardiogram to predict dyskalaemias in patients with multiple visits. *Eur. Heart J. Digit. Health*. **4**, 22-32 (2023,1)
- Ahn, J., Attia, Z., Rattan, P., Mullan, A., Buryska, S., Allen, A., Kamath, P., Friedman, P., Shah, V., Noseworthy, P. & Simonetto, D. Development of the AI-cirrhosis-ECG score: An electrocardiogram-based deep learning model in cirrhosis. *Am. J. Gastroenterol.* **117**, 424-432 (2022,3)
- Rafie, N., Kashou, A. & Noseworthy, P. ECG interpretation: Clinical relevance, challenges, and advances. *Hearts (Basel)*. **2**, 505-513 (2021,11)
- O'Shea, K. & Nash, R. An Introduction to Convolutional Neural Networks. (arXiv,2015)
- Sherstinsky, A. Fundamentals of recurrent neural network (RNN) and long short-term memory (LSTM) network. *Physica D*. **404**, 132306 (2020,3)
- Zhu, H., Xu, J., Liu, S. & Jin, Y. Federated learning on non-IID data: A survey. *Neurocomputing*. **465** pp. 371-390 (2021,11)
- Prayitno, Shyu, C., Putra, K., Chen, H., Tsai, Y., Hossain, K., Jiang, W. & Shae, Z. A systematic review of federated learning in the healthcare area: From the perspective of data properties and applications. *Appl. Sci. (Basel)*. **11**, 11191 (2021,11)
- Sadilek, A., Liu, L., Nguyen, D., Kamruzzaman, M., Serghiou, S., Rader, B., Ingerman, A., Mellem, S., Kairouz, P., Nsoesie, E., MacFarlane, J., Vullikanti, A., Marathe, M., Eastham, P., Brownstein, J., Arcas, B., Howell, M. & Hernandez, J. Privacy-first health research with federated learning. *NPJ Digit. Med.* **4**, 132 (2021,9)
- Brás, S., Ferreira, J., Soares, S. & Pinho, A. Biometric and emotion identification: An ECG compression based method. *Front. Psychol.* **9** (2018,4)
- Melzi, P., Tolosana, R. & Vera-Rodriguez, R. ECG biometric recognition: Review, system proposal, and benchmark evaluation. *IEEE Access*. **11** pp. 15555-15566 (2023)
- Ji, Z., Lipton, Z. & Elkan, C. Differential privacy and machine learning: A survey and review. (arXiv,2014)
- Zoonen, L. Privacy concerns in smart cities. *Gov. Inf. Q.* **33**, 472-480 (2016,7)
- Dwork, C. Differential Privacy. *Automata, Languages And Programming*. pp. 1-12 (2006)
- McMahan, B., Moore, E., Ramage, D., Hampson, S. & Arcas, B. Communication-Efficient Learning of Deep Networks from Decentralized Data. *Proceedings Of The 20th International Conference On Artificial Intelligence And Statistics*. **54** pp. 1273-1282 (2017,4,20), <https://proceedings.mlr.press/v54/mcmahan17a.html>
- Raza, A., Tran, K., Koehl, L. & Li, S. Designing ECG monitoring healthcare system with federated transfer learning and explainable AI. *Knowl. Based Syst.* **236**, 107763 (2022,1)
- Moody, G. & Mark, R. The impact of the MIT-BIH arrhythmia database. *IEEE Eng. Med. Biol. Mag.* **20**, 45-50 (2001,5)
- Tang, R., Luo, J., Qian, J. & Jin, J. Personalized federated learning for ECG classification based on feature alignment. *Secur. Commun. Netw.* **2021** pp. 1-9 (2021,11)
- Goto, S., Solanki, D., John, J., Yagi, R., Homilius, M., Ichihara, G., Katsumata, Y., Gaggin, H., Itabashi, Y., MacRae, C. & Deo, R. Multinational federated learning approach to train ECG and echocardiogram models for hypertrophic cardiomyopathy detection. *Circulation*. **146**, 755-769 (2022,9)
- Lin, D., Guo, Y., Sun, H. & Chen, Y. FedCluster: A Federated Learning Framework for Cross-Device Private ECG Classification. *IEEE INFOCOM 2022 - IEEE Conference On Computer Communications Workshops (INFOCOM WKSHPS)*. pp. 1-6 (2022)
- Meqdad, M., Hussein, A., Husain, S. & Jawad, A. Classification of electrocardiogram signals based on federated learning and a gaussian multivariate aggregation module. *Indones. J. Electr. Eng. Comput. Sci.* **30**, 936 (2023,5)
- Baumgartner, M., Veeranki, S., Hayn, D. & Schreier, G. Introduction and comparison of novel decentral learning schemes with multiple data pools for privacy-preserving ECG classification. *J. Healthc. Inform. Res.* **7**, 291-312 (2023,9)
- Yin, X., Zhu, Y. & Hu, J. A comprehensive survey of privacy-preserving federated learning. *ACM Comput. Surv.* **54**, 1-36 (2022,7)
- Yousefpour, A., Shilov, I., Sablayrolles, A., Testuggine, D., Prasad, K., Malek, M., Nguyen, J., Ghosh, S., Bharadwaj, A., Zhao, J., Cormode, G. & Mironov, I. Opacus: User-Friendly Differential Privacy Library in PyTorch. *ArXiv Preprint ArXiv:2109.12298*. (2021)
- Mironov, I. Rényi Differential Privacy. *2017 IEEE 30th Computer Security Foundations Symposium (CSF)*. pp. 263-275 (2017)
- Mironov, I., Talwar, K. & Zhang, L. Rényi differential privacy of the Sampled Gaussian Mechanism. (arXiv,2019)
- Shokri, R., Stronati, M., Song, C. & Shmatikov, V. Membership Inference Attacks Against Machine Learning Models. *2017 IEEE Symposium On Security And Privacy (SP)*. pp. 3-18 (2017)
- PhysioNet George B. Moody PhysioNet Challenge. (2020,3), <https://moody-challenge.physionet.org/2020/>
- Ying, Z., Zhang, G., Pan, Z., Chu, C. & Liu, X. FedECG: A federated semi-supervised learning framework for electrocardiogram abnormalities prediction. *J. King Saud Univ. - Comput. Inf. Sci.* **35**, 101568 (2023,6)
- Joshi, M., Pal, A. & Sankarasubbu, M. Federated learning for healthcare domain - pipeline, applications and challenges. *ACM Trans. Comput. Healthc.* **3**, 1-36 (2022,10)
- Dolo, B., Loukil, F. & Boukadi, K. Early Detection of Diabetes Mellitus Using Differentially Private SGD in Federated Learning. *2022 IEEE/ACS 19th International Conference On Computer Systems And Applications (AICCSA)*. pp. 1-8 (2022)
- Abadi, M., Chu, A., Goodfellow, I., McMahan, H., Mironov, I., Talwar, K. & Zhang, L. Deep learning with differential privacy. *Proceedings Of The 2016 ACM SIGSAC Conference On Computer And Communications Security*. (2016,10)
- Sun, W., Kalmady, S., Sepehrvand, N., Salimi, A., Nademi, Y., Bainey, K., Ezekowitz, J., Greiner, R., Hindle, A., McAlister, F., Sandhu, R. & Kaul, P. Towards artificial intelligence-based learning health system for population-level mortality prediction using electrocardiograms. *NPJ Digit. Med.* **6**, 21 (2023,2)
- Bradley, A. The use of the area under the ROC curve in the evaluation of machine learning algorithms. *Pattern Recognit.* **30**, 1145-1159 (1997,7)
- Ponomareva, N., Hazimeh, H., Kurakin, A., Xu, Z., Denison, C., McMahan, H., Vassilvitskii, S., Chien, S. & Thakurta, A. How to DP-fy ML: A practical guide to machine Learning with differential privacy. *J. Artif. Intell. Res.* **77** pp. 1113-1201 (2023,7)
- Tenison, I., Sreeramadas, S., Mugunthan, V., Oyallon, E., Rish, I. & Belilovsky, E. Gradient masked averaging for federated learning. (arXiv,2022)
- Hong, M., Kang, S. & Lee, J. Weighted averaging federated learning based on example forgetting events in label imbalanced non-IID. *Appl. Sci. (Basel)*. **12**, 5806 (2022,6)

[43] Xiao, P., Cheng, S., Stankovic, V. & Vukobratovic, D. Averaging is probably not the optimum way of aggregating parameters in federated learning. *Entropy (Basel)*. 22, 314 (2020,3)

[44] Agarap, A. Deep Learning using Rectified Linear Units (ReLU). (arXiv,2018)

[45] Ioffe, S. & Szegedy, C. Batch Normalization: Accelerating deep network training by reducing internal covariate shift. (arXiv,2015)

[46] Kingma, D. & Ba, J. Adam: A method for stochastic optimization. (arXiv,2014)

[47] Association, A. Privacy Policy. (2023,6), <https://www.aha.org/2022-07-14-privacy-policy>

[48] American Medical Association Code of Medical ethics. (2016), <https://code-medical-ethics.ama-assn.org/>

[49] Disease Control, C. & Prevention Health Insurance Portability and Accountability Act of 1996. (1996), <https://www.cdc.gov/phlp/publications/topic/hipaa.html>

A APPENDIX

Table 6 contains the ICD-10 codes and their corresponding disease names for our classification labels.

Table 6: ICD-10 codes used and their disease names

ICD-10 Code	Disease Name
I21.1	ST elevation (STEMI) myocardial infarction of inferior wall
I21.0	ST elevation (STEMI) myocardial infarction of anterior wall
I50.0	Heart failure
I25.10	Atherosclerotic heart disease of native coronary artery without angina pectoris
I48.9	Unspecified atrial fibrillation and atrial flutter
I21.4	Non-ST elevation (NSTEMI) myocardial infarction
I48.0	Paroxysmal atrial fibrillation
E87.5	Hyperkalemia
E11.2	Type 2 diabetes mellitus with kidney complications
I35.0	Nonrheumatic aortic (valve) stenosis

Figures 7 and 8 depict label-wise model performance across various testing sites. Figure 7 illustrates the model performance for the Standard Approach, whereas Figure 8 showcases the model performance for the Federated Learning Approach.

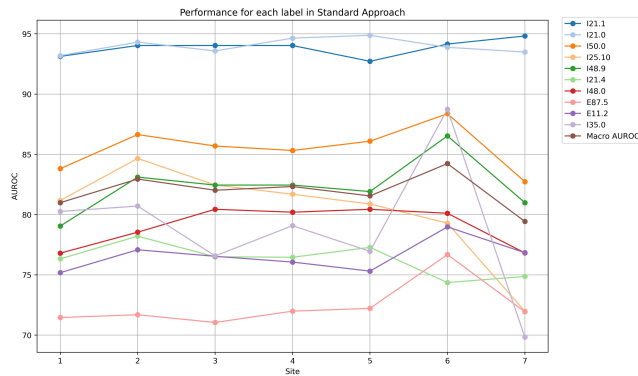


Figure 7: Plot shows model performance (AUROC in %) for each label as well as the Macro AUROC using the Standard Approach

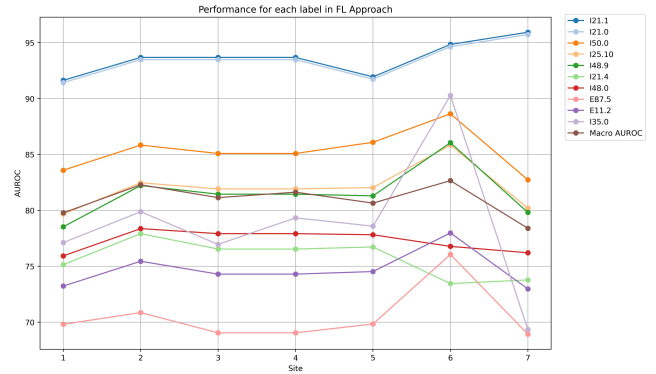


Figure 8: Plot shows model performance (AUROC in %) for each label as well as the Macro AUROC using the Federated Learning Approach